
Article:
Alsaadi, A., Meredith, J., Swait, T. et al. (2 more authors) (2019) Damage detection and location in woven fabric CFRP laminate panels. Composite Structures, 220. pp. 168-178. ISSN 0263-8223

https://doi.org/10.1016/j.compstruct.2019.03.087

Damage Detection and Location in Woven Fabric CFRP Laminate Panels

(https://doi.org/10.1016/j.compstruct.2019.03.087)

A. Alsaadi[a,*], J. Meredith[b], T. Swait[c], J. L. Curiel-Sosa[d], S. Hayes[e]

[a]*Department of Materials Science and Engineering, Sir Robert Hadfield Building, Mappin Street, Sheffield S1 3JD, UK*

[b]*WMG, The University of Warwick, Coventry, CV4 7AL*

[c]*Composite Centre, Advanced Manufacturing Research Centre, University of Sheffield, Wallis Way, Catcliffe, S60 5TZ*

[d]*Department of Mechanical Engineering, University of Sheffield, Sir Frederick Mappin, Mappin St, Sheffield S1 3JD, UK*

[e]*Department of Multidisciplinary Engineering Education The University of Sheffield 32 Leavygreave Road Sheffield S3 7RD*

Abstract

The need for multifunctional carbon fibre composite laminates has emerged to improve the reliability and safety of carbon fibre composite components and decrease the cost. The development of an electrical self–sensing system for *woven fabric* carbon fibre composite laminate panels which can detect and locate damage due to impact events is presented. The electrical sensing system uses a four – probe electrical resistance method. Two different sensing mats are investigated, the main difference between them are the surface area of the electrodes and the distance between the electrodes. To investigate the damage sensitivity of the sensing system for woven fabric carbon fibre composite laminate panels, panels are produced with various thicknesses from 0.84 – 3.5 mm and are impacted at 1 – 10 J to generate barely visible impact damage. Damage is detected using global electrical resistance changes, the changes in electrical resistance vary depending on carbon fibre volume fraction, spacing distance between the sensing electrodes in the sensing mats, the surface area of the electrodes, damage size, and damage type; it is found that the thicker the panel, the less sensitive the electrical resistance system is. The effect of the surface area of the sensing elec-

*Corresponding author: Ahmed Al-Saadi (a.alsaadi@sheffield.ac.uk)

trodes is high on the electrical resistance baseline, where the baseline increases by up to 55 % when the surface area of the sensing electrodes increases from 100 mm^2 to 400 mm^2; while spacing distance between electrodes has a greater effect on damage sensitivity of the electrical resistance sensing system than the surface area of the sensing electrodes.

Keywords: `Carbon fibre composites, electrical self - sensing, damage detection, damage location`

2018 MSC: 00-01, 99-00

---

1. Introduction

Smart sensing composite systems have potential to reduce the cost of the maintenance, turnaround time and safety factors in many composite applications [1]. These systems have experienced a growing interest from different industries [2, 3, 4, 5, 6]; in particular the aerospace industry [7], where high operational safety factors, minimisation of downtimes and reduction of structural inspection costs are required [8]. For large composite structures, knowing the damage location and severity are desirable [9]. Different types of damage such as delamination, matrix cracking and fibre breakage can be detected using different sensing techniques, such as fibre optic, acoustic, thermography or electrical sensing techniques [10, 11, 12, 13, 14, 15]. Sensing techniques may differ in terms of expense, level of instrumentations, accuracy and robustness required.

The sensing systems either incorporate sensors into the composite structures such as Fibre Bragg gratings (FBG) or attach or insert sensors into the composite structures such as acoustic methods and Fabry Perot Interferometer (FPI) [14, 16, 17, 18]. Once those sensors have been integrated into the composite structures a new challenge will have to be overcome; establishing a relationship between changes in the physical properties of the sensors and changes in properties of the composite structures being monitored, such as temperature, pressure, mass, stiffness etc.

An alternative way, which may be more natural, to obtain a smart material is to use composite material constituents as a sensor [19, 20, 21, 22]. This is highly possible in carbon fibre reinforced polymers (CFRP) since they consist at least two elements; carbon fibre which is highly conductive (its conductivity is 1500 S /m and matrix that is highly insulating, (for example the electrical conductivity of the epoxy matrix is 10^{-11} S /m to 10^{-13} S /m. The directionality in electrical properties of CFRP laminates was deployed to investigate damage [23, 24, 25, 26] or monitor strain [27, 28, 29, 30]. The electrical resistance change technique has advantages over other methods since it employs the carbon fibre itself as a sensor to measure the changes in electrical resistance and consequently monitors strain and/or detects damage directly.

The features (i.e. strain monitoring, damage monitoring, and damage detection) determine the type of electrical current being used [31]. Direct current (DC) is suitable to monitor fibre fracture and delamination process, since those types of damage produce a measurable change in electrical resistance [32, 33]. While alternating current (AC) is mainly used to monitor resin infusion process during liquid moulding processes and thermoset resin cure based on dielectric analysis. In practice CFRP structures are subject to different types of loading. While CFRP has shown excellent resilience for most types of loads, it can be vulnerable to impact events. Internal damage (such as delamination which is difficult to detect using conventional methods) maybe generated under low impact energies and cause a significant reduction in the mechanical properties [34], which in turn may lead to catastrophic failure.

Extensive research over the last few years has been undertaken to study the electrical sensing techniques in unidirectional, cross-ply, and quasi-isotropic CFRP laminates, but there has been a limited research that has applied this technique on woven fabric CFRP laminates, that is due to complexity of current flow in woven fabric CFRP laminates. Also the vast majority of previous research was investigated the electrical resistance sensing technique on a bar-type specimen, therefore this paper is extending the use of electrical resistance sensing system to the woven fabric CFRP laminates using a panel-type spec-

imen. An innovative sensing mats were used to detect and locate damage in woven fabric CFRP laminate due low velocity impact events. Global electrical resistance changes were used to detect damage in the panels; a simple analytical method was used to locate damage. The effects of all pertinent aspects from fibre volume fraction, spacing between sensing electrodes, surface area of sensing electrodes, and panel thicknesses to damage size and type on the sensing system was studied. Then an optimisation study was performed on the sensing system toward being a viable alternative for expensive non - destructive testing (NDT) techniques.

2. Methodology

2.1. Materials and Fabricating Techniques

CFRP panels were fabricated using an autoclave processing technique. The CFRP panels made at various thicknesses these being 0.84, 1.63, 2.54, and 3.5 mm; all the panels were fabricated from a single prepreg lot and their stacking sequence was $(0F)_4, (0F)_8, (0F)_{12}, (0F)_{16}$ respectively, where F refers to fabric weave carbon fibre. Carbon fibre VTC 401 prepreg (SHD Composite Materials, UK) was used to make the panels, this prepreg uses a 2 x 2 mm twill weave fabric of Toray FT300B carbon fibre. A single - sided composite laminate sheet, Pyralux FR8510R (Dupont, USA), that consists of 15 µm of copper foil bonded to a 25 µm thick of flexible film of polyimide was used to make the sensing mats. The sensing mats were produced using a standard photo - lithoraphic technique, the sensing mats patterns are shown in Figure 1. A cover layer was used to isolate tracks in the sensing mats from making contacts with the carbon fibre panels this being Pyralux FR 0110 Coverlay (Dupont, USA). The coverlay of 25 µm was applied to the top surface of the sensing ply to isolate the tracks from making connections with the CFRP laminate as shown in Figure 2.

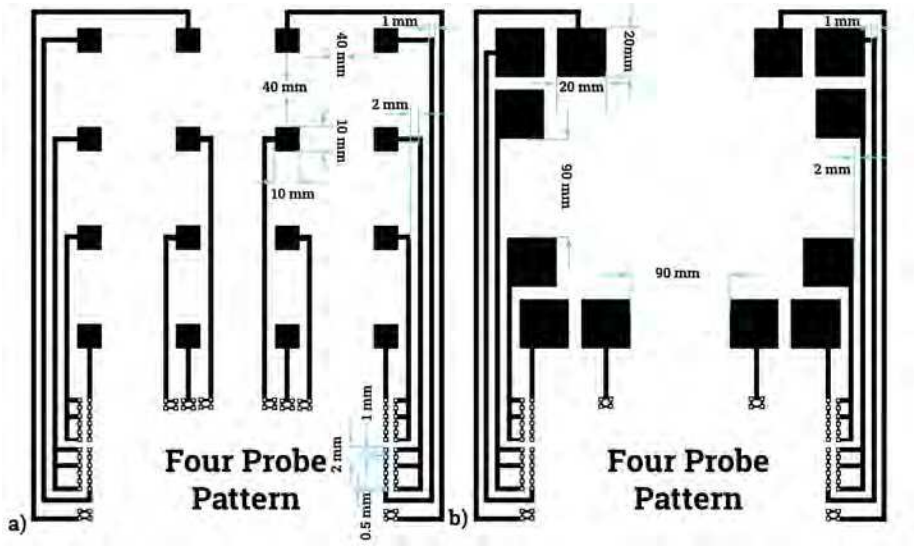

Figure 1: Sensing mats patterns designed using Photoshop CC 2017 (Adobe, USA) a) sensing mat 1 and b) sensing mat 2.

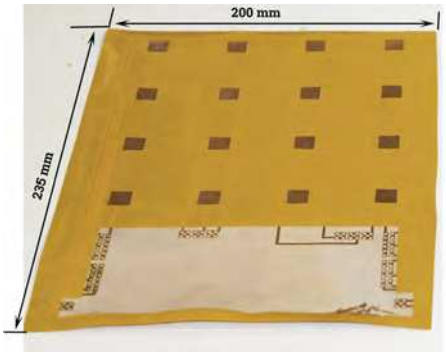

Figure 2: Ready to use sensing mat 1.

2.2. Fibres Volume Fraction Measurements

To measure the carbon fibre volume fraction, three specimens 18 x 18 x t mm (t is the panel thickness 0.84, 1.63, 2.54, and 3.5 mm) were cut using 3000 rpm diamond saw and the linear velocity being adjusted manually. A density measurement device (Mettler Toledo-Newclassic MS. Model MS104S/01, UK) was used to measure the relative density of the carbon fibre composite laminates

according to ASTM D792 – 13. Each specimen was placed in a flask that contains at least 30 mL of 70 % nitric acid. The flask was placed in an oil bath and they were placed on a hot plate ASTM D3171-15. It was found that the optimum digestion time is 120 minutes when the temperature was maintained at $80^oC \pm 2$. Once digestion was complete the specimen was taken out of the flask, filtered into pre-weighed sintered glass filter under a vacuum of 1 bar. The carbon fibres were then washed using distilled water then placed in an air-circulation oven (Heratherm, Thermoscientific, USA) to dry at 50^oC for 90 minutes. Then the specimens were weighed to nearest 0.0001 g. The specimen was dried again in the oven and re-weighed after 90 minutes, and the process continues until constant mass was reached. The following formula was used to calculate fibre, resin and void contents respectively:

$$\phi_f = (w_f \cdot \rho_c)/\rho_f \tag{1}$$

Where ϕ_f is the fibre volume fraction %, w_f is fibre mass (g), and ρ_f is carbon fibre filament density that is 1.8 g/cm^3.

2.3. Microscopical Examination of CFRP Panels

A Nikon Eclipse LV-150 reflected-light microscope was used to examine the CFRP panels. The panels were sectioned in z-axis (through – thickness direction) to a manageable size 18 x 18 x t mm, where t is the specimens thickness that is 0.84, 1.63, 2.54, and 3.5 mm respectively. The sectioning was undertaken using a diamond cutter in the presence of water (the water was used as a cutting fluid and coolant at the same time) to maintain the temperature of the specimens at room temperature and to avoid creating or altering the artefacts of the specimen. A standard preparation method provided by (Buehler, Germany) was adopted to polish the specimen. Epi-fluorescent microscopy was also used to examine matrix cracks, delamination and intralaminar cracks in CFRP panels. representative areas were cut from the impacted panels. To achieve greater contrast between the micro-cracks, macro-cracks and other features, a fluorescent dye EpoDye (Struers, Demark) was mixed with the mounting resin

Epofix (component A) prior to adding the harder (component B) to the resin. This dye will fluoresce under the UV-light, therefore, it provides high contrast to distinguish between various types of features in the panels.

2.4. Self - Sensing Laminates

A good quality electrical contact between the CFRP panels and the sensing mats is necessary for electrical sensing analysis. A rough grinding for carbon fibre laminates was required to remove the artefacts that are formed due to the peel ply surface finish. The rough grinding step is essential to remove the epoxy layer from the surface that will be in contact with the sensing mat. The samples were then ground using 240, and 600 grit silicon carbide (SiC) papers (Metprep, UK) and polished by using 1200 grit silicon carbide papers (Metprep, UK). A cleaning grade of isopropyl alcohol (Sigma Aldrich, UK) was used to remove any particulates from the surface. A 10X magnifier (Zeiss, UK) was used to ensure that the epoxy was removed from the targeted area.

The grinding and polishing procedure were undertaken by hand since the size of the sample helps to do it manually rather than using automated grinding machines. To maintain a high-quality flat surface the sample held from one side by one hand and the grinding step starts from one side all the way up to the other side repeatedly in warp then in weft direction consecutively. Then the sample was washed with water then dried in the air, then washed using isopropyl alcohol between each stage. Figure 3 shows the final samples before attaching the sensing mat to the panels.

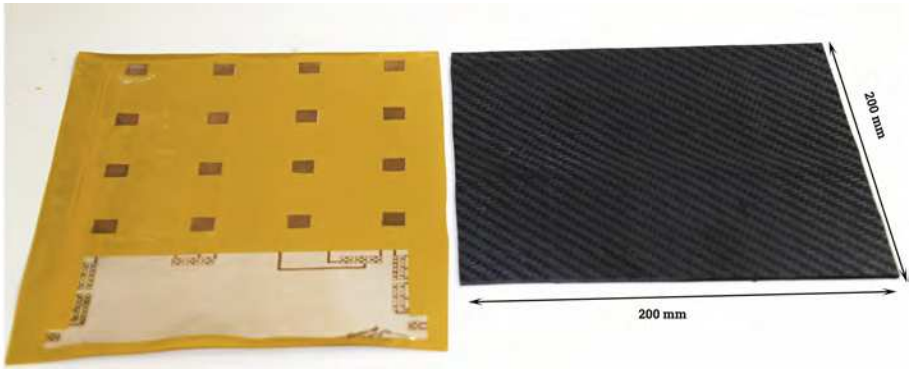

Figure 3: Graphs showing the finish of the same panel before and after abrasion process

The sensing mats were attached to the CFRP panels using Silver-Epoxy room temperature curing conductive adhesive 8331S (MG Chemicals, UK), with a high thermal conduction 10 W/(m.K), and low resistivity 0.0010 $\Omega.cm$. A small quantity of epoxy silver paste was placed carefully on the electrodes (1 g on each electrode in sensing mat 1 and 1.5 g on each electrode in sensing mat 2). Care was taken to ensure all the electrodes were covered with the same amount of the epoxy silver paste. Then the panels were placed onto the sensing mats and were enveloped in a vacuum bag. 101 kPa of vacuum pressure was applied inside the vacuum bag for 24 hours to ensure good electrical contacts between them and the sensing mats. Then the panels were taken out of the vacuum bag for further processing. It is found that the panels were able to undergo further handling and testing when they had been left under the vacuum pressure for 24 hours. The smart carbon fibre composite laminate panel is shown in Figure 4.

Figure 4: Self - sensing composite laminate panel.

2.5. Damage Generation and Electrical Resistance Measurements

Barely visible impact damage (BVID) was generated using drop – weight impact tester according to ASTM D7136/D7136M-15. Where a flat composite panel 200 x 200 x t mm (t = 0.84, 1.63, 2.54, and 3.5 mm) is subjected to through-thickness concentrated impact energy. The weight (1.456 kg) was dropped from pre-determined heights. Various heights were used, these being 70, 105, 140, 245, 375 and 700 mm, to strike the CFRP laminate panel. A hemi-spherical impactor, 13 mm in diameter, was used. The carbon fibre composite laminate panel was supported on the horizontal plane using G-clamps, the impact energies are shown in Table 1.

Table 1: Experimental data of low velocity impact energy and damaged area that was measured using C-scan. 13 mm round impact tip was used to generate damage.

Specimen	Incident Energy (J)	Incident Velocity (m/s)	Damage Area (mmˆ2)
AB	1	1.17	61.6
	1.5	1.43	100.06
	2	1.65	122.01
	3.5	2.19	400.13
	5	2.6	654.06
AC	2	1.65	122.01
	3.5	2.19	400.13
	5	2.6	654.06
AD	5	2.6	200.36
	10	3.7	293.52
AE	5	2.6	200.36
	10	3.7	293.52

To measure the electrical resistance of CFRP panels, the current sensing system adopts modules of NI9219 (National instrument, US) installed in a NI cDAQ-9172 (National instruments, US) chassis. NI9219 was set up to four-probe electrical resistance configuration. In the four-probe technique the contacts resistance (pin headers, soldering materials, and connection wires) are neglected since there is only a small amount or none of electrical current flowing across the electrical potential terminals. The four - probe electrical resistance technique is also more sensitive, accurate and more precise than the two-probe method in sensing impact damage in CFRPs [29]. It is proved elsewhere that it can present a subsurface behaviour [26]. The terminals in NI9219 modules were energised consecutively to avoid the interference between a terminal and the others during the data collection process.

2.5.1. Through - Thickness Electrical Resistivity

A 200 x 200 x t mm CFRP panels were used, where t represents the thickness of the CFRP panels that being 0.84, 1.63, 2.54, and 3.5 mm. The laminates were ground and polished as described in Section 2.4 prior to attach the sensing mats. Two sensing mats were attached to each CFRP panel (one to the upper surface and the other to the lower surface of the CFRP panel). To measure through-thickness electrical resistance a direct electrical current of 500 μA flows through-thickness from the upper side (I_{in}) to the lower surface (I_{out}) of the CFRP panel and the voltage measurements were taken as shown in Figure 5.

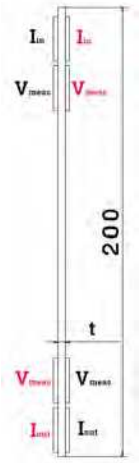

Figure 5: Schematic diagram illustrates the experimental set up to measure through – thickness electrical resistance, unit is mm.

This process was reversed, the current flows through-thickness of the CFRP panel from the lower surface to the upper surface, for one main purpose that is to acquire more electrical resistance readings at a shorter time. 10 electrical resistance readings were taken and the average values were considered in further calculations. The through - thickness electrical resistivity of the panel (η_t) was calculated using the following equation

$$\eta_t = R \cdot (A/L) \tag{2}$$

Where R is the electrical resistance (Ω), A is the surface area of the electrode (mm^2), L is the distance between the voltage electrodes (mm). Equation 2 was used to calculate the distance between the electrodes

$$L = \sqrt{t^2 + b^2} \tag{3}$$

Where t is the thickness of the panels (mm), and b is 60 mm for sensing mat 1 and 130 mm for sensing mat 2. The angle between the voltage electrodes on the upper and lower surface was calculated using Equation 4

$$\tan\theta = (t/b) \tag{4}$$

Therefore, θ was 0.8, 1.55, 2.42, and 3.33^o for 0.84, 1.63, 2.54, and 3.5 mm panels using sensing mat 1 and θ was 0.37, 0.71, 1.11, and 1.54^o for panels 0.84, 1.63, 2.54, and 3.5 mm panels using sensing mat 2.

The electrical conductivity of the composite (C_c) is a fundamental property that determines the ability of a material to allow the flow of the electrical current. The electrical conductivity of composite (C_c) was calculated for each carbon fibre composite laminates panels that were used in this work Table **??**. The rule of mixture was used to calculate the electrical conductivity (C_c) in the carbon fibre composite laminates panels. Equation 5 describes the relationship between C_c of composites and their constituents

$$C_c = C_f.V_f + C_m.(1 - V_f) \tag{5}$$

Where C_f is the electrical conductivity of the carbon fibre (carbon fibre filaments), the electrical resistivity of Toray FT300B carbon fibre is $1.7x10^{-2}\Omega$.mm, where the electrical conductivity is the reciprocal of electrical resistivity. V_f is the fibre volume fraction, C_m is the electric conductivity of the epoxy matrix. The epoxy matrix is an insulator, therefore C_m is vanished and the rule of mixture equation will be simplified to Equation 6:

$$C_c = C_f.V_f \tag{6}$$

Table 2: Through – thickness electrical conductivity of composites at various carbon fibre volume fractions.

Thickness	0.84	1.63	2.54	3.5
Vf%	44.27	50.67	54.35	54.44
Cc (Ohm.mm)ˆ-1	2604.117	2980.588	3197.058	3202.352

2.5.2. Surface Electrical Resistance

The measurements of the surface electrical resistance were taken; a 500 μA DC was injected into the CFRP panels using sensing mats that were attached to the bottom surface as shown in Figure 6. 10 electrical resistance readings were taken of each electric channel (A1, A2, A3, A4, B1, B2, B3 and B4) and the average values were considered in further calculations.

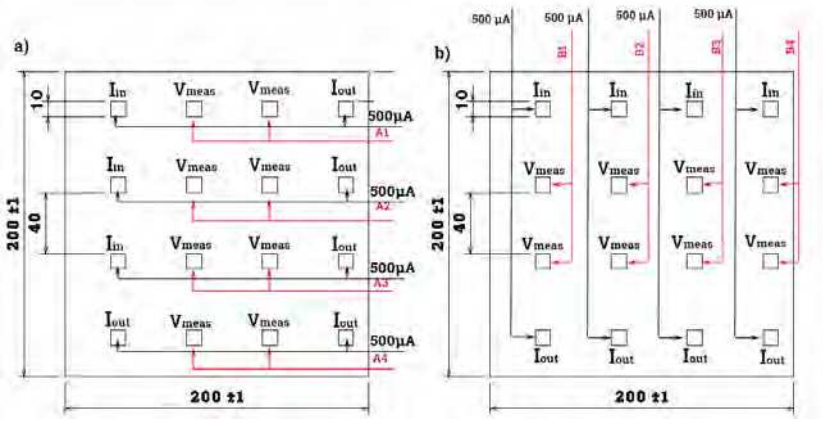

Figure 6: Dependence of through – thickness electrical resistivity of carbon fibre composite laminates panels on thickness and fibre volume fraction. The electrical resistivity was measured using both sensing mat 1 and sensing mat 2.

It was found that increasing the contacts area from 100 mm^2 (mat 1) to 400 mm^2 (mat 2) increased the baseline electrical resistances up to $\simeq$ 55%, this occurs due to the decrease in the current density and the increase in the distance between the electrodes from 40 mm to 90 mm. It was also found that the change in the baseline electrical resistance over time was minimal, showing

the robustness of the four-probe electrical resistance method compared to other electrical sensing methods.

The global electrical resistance change refers to the whole change in electrical resistance of the CFRP panels due to damage. Equation 7 and Equation 8 were used to calculate the global electrical resistance change for the carbon fibre composite laminate panel.

$$\xi_1 = \frac{\sum_{A1}^{A4}(\Delta R/R_o) + \sum_{B1}^{B4}(\Delta R/R_o)}{8} \tag{7}$$

$$\xi_2 = \frac{\sum_{A1}^{A2}(\Delta R/R_o) + \sum_{B1}^{B2}(\Delta R/R_o)}{4} \tag{8}$$

2.6. Non-destructive testing

The damage profile and the damaged area were investigated using a C-scan camera (DolphiCam, UK). To calculate the damaged area, the C – scan images were imported to Adobe Photoshop CC 19.1.5 (Adobe, US). Total number of pixels of C - scan transducer pad was counted and it was found 40716 pixel, and then number of pixels in the damaged region was counted. The percentage of the damaged area to the total area of the C – scan transducer pad was calculated by dividing the number of pixels of the damaged area by the whole C – scan transducer pad's pixels. The C – scan transducer pad area was known that was $900mm^2$. Therefore, the damaged areas were calculated by multiplying $900mm^2$ by the percentage of damaged area, therefore the damaged areas were presented in Table 1.

3. Results and Discussions

3.1. Through - Thickness Electrical Resistivity

Figure 7 shows through - thickness electrical resistivity measured using the experimental set ups described in Section 2.5.1 using both sensing mats shown in Figure 1.The effect of panel thickness and the fibre volume fraction on the through - thickness electrical resistivity can be seen. It can be seen in Figure 7

that increasing carbon fibre volume results in a decrease in through - thickness electrical resistivity. This was expected as a higher volume fraction increased the number of fibre - fibre contacts between adjacent plies due to the waviness of carbon fibre (Figure 8). Disruption of these fibre-fibre contacts was the basis for the ability of the resistance measurement to detect damage.

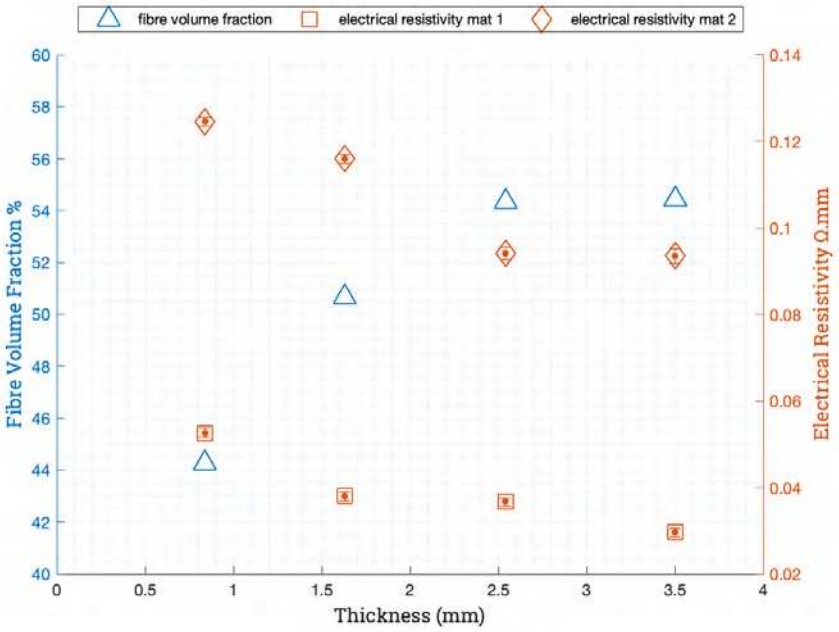

Figure 7: Electrical resistance measurements using sensing mat 1 a) electrical resistance along 0^o and b) electrical resistance along 90^o, unit is mm.

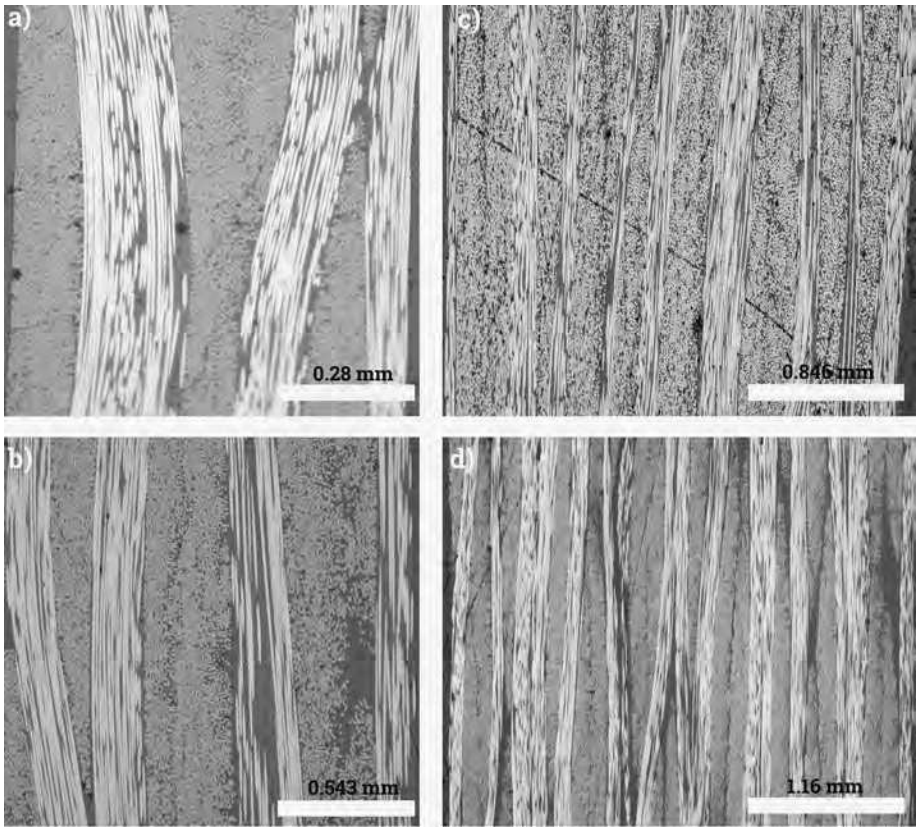

Figure 8: Montage of optical microscopic images for cross-section of a carbon fibre composite laminate panels that were made from prepreg VTC401 by using an autoclave processing technique. The electrical contacts between adjacent plies occurred due to fibre – fibre contacts that can be seen in all images, a) 0.84 mm panel, b) 1.63 mm panel, c) 2.54 mm panel, and d) 3.5 mm panel.

The baseline of the through - thickness electrical resistivity decreased when the panel thickness increased which was expected given the thicker panels had higher V_f. The electrical resistivity increased by up to 55 % when measured using sensing mat 2, that due to electrode size and the sensing length that were $400\,mm^2$ and 90 mm for sensing mat 2 and $100\,mm^2$ and 40 mm for sensing mat 1. However, sensing mat 2 was less sensitive for damage detection than sensing mat 1 as discussed in Section 3.2. It can be seen in Figure 7 that there was no changes in electrical resistivity curve in the region between 2.54 and 3.5 mm that

means that sensing mat 2 was not able to measure the reduction in electrical resistivity due to increase in fibre volume fraction. The electrical conductivity followed the same pattern where it increased when the carbon volume fraction increased as shown in Figure 9.

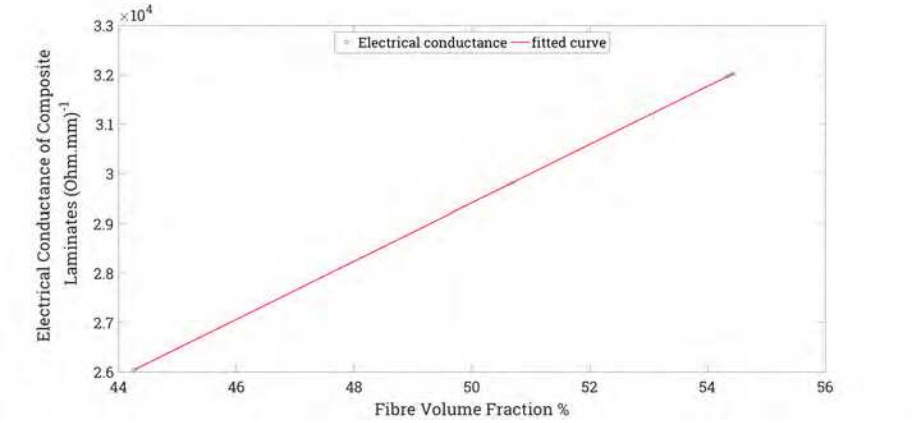

Figure 9: Calculated electrical conductance of carbon fibre composite laminates.

3.2. Damage Detection

The sensitivity of the sensing system to detect BVID in CFRP panels was investigated using a range of impact energies as shown in Figure 10. Those energies were selected so as to cause BVID. In Figure 10 sensing mat 1 was attached to the bottom surface of the panels, while impact energies were applied on upper surface of the panels. The bar chart in Figure 10 shows that there is a positive correlation between the changes in global electrical resistance ξ of the panels and the impact energies. Fundamentally, the amount of changes in electrical resistance dependes on the panels thicknesses, the fabricating process, the epoxy matrix, the impact energies, and the sensing mat.

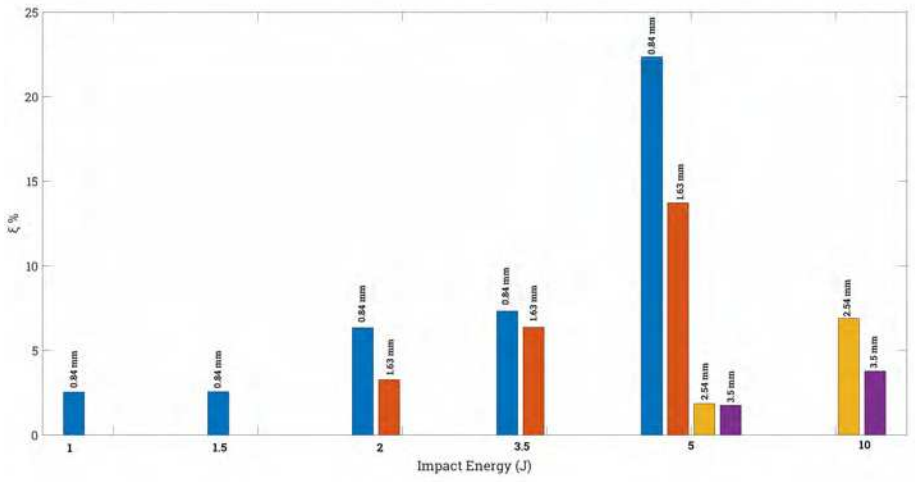

Figure 10: The percentage change in electrical resistance in carbon fibre composite laminate panels due to impact damage using sensing mat 1. Number on the bars represent panel thicknesses.

When 1 J of impact energy was applied on the panels, it was noticed that BVID was created in the 0.84 mm panel, while the other panels were not affected by that amount of impact energy. When the impact energy increased to 2 J, all the panels apart from 2.54 and 3.5 mm panel showed signs of damage Table 1. The amount of changes in electrical resistance varied depending on the size of damage and that in turn differed due to size effect, where at a given impact energy the severity of damage decreased as panel thickness increased. Table 1 shows that for example at 2 J of impact energy the 0.84 mm panel showed a bigger damage size than 1.63 mm panel (122.01 and 71.68 mm^2 respectively). The damage in 0.84 mm panel was a combination of matrix cracks, delamination and fibre breakage, where the impact energy exceeded the impact energy required to cause fibre rupture. The energy required to cause a fibre rupture is presented in Table 3.

Table 3: The impact energies required to cause fibre failure due to back surface flexure.

Thickness (mm)	0.84	1.63	2.54	3.5
Energy (J)	1.95	4.15	9.92	14.21

The fibre breakage was observed on the bottom surface due to tensile loads on that surface. However, 1.63 mm panel showed only matrix cracks and delamination and no fibre breakage was observed as shown in Figure 11. The highest electrical resistance change was observed in the 0.84 mm panels. It is expected that the void content in all panels have a minor impact on the electrical resistance since it is less than 2%. It was noticed that when the impact energy level was below the threshold in Table 3, the dominant form of damage is delamination and matrix cracks, therefore the change in electrical resistance is relatively low. However, when the impact energy exceeds the threshold energy a considerable change in electrical resistance was observed as shown in Figure 10, since all types of damage; fibre breakage, delamination and matrix cracking, occur. When the panels were subjected to 3.5 J of impact energy, fibre failure was observed in 0.84 mm panel. Fibres ruptured on the bottom surface of the panel, since the bottom surface was subject to tension and the upper surface to compression due to global bending loads. The damage was classified as a visible damage, while the damage in 1.63 mm panel was smaller in size and less in severity, therefore, it was classified as barely visible although as can be seen in Figure 11, an extensive delamination occurred between almost every ply.

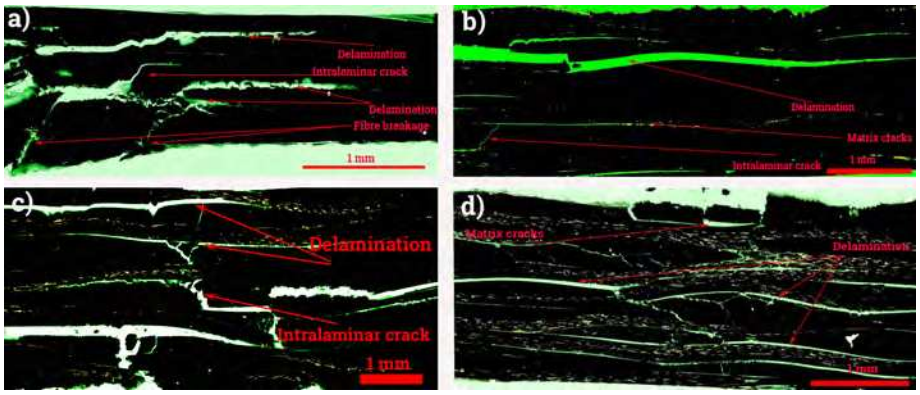

Figure 11: Montage of fluorescent microscope images of impact damage of 0.84 and 1.63 mm panels that impacted at various impact energies a) 0.84 mm panel that was impacted at 2J, b) 1.63 mm panel that was impacted at 2 J, c) 1.63 mm panel that was impacted at 3.5 J, d) 1.63 mm panel that was impacted at 5 J.

5 J of impact was caused significant changes in electrical resistances in the impacted regions of 0.84 mm and 1.63 mm panels, however, the damage was smaller in 2.54 mm and 3.5 mm panels. The impactor perforated the 0.84 mm panel, this led to a high increase in electrical resistance $\approx 23\%$. In addition to matrix cracks and delamination, this impact energy caused fibre breakage in the 1.63 mm panel as shown in Figure 11. Fibre breakage was not observed in all other panels. 5 J of impact energy created damage areas of 200.46 and 170.36 mm^2 in AD and AE panel respectively, however, it was found that the electrical resistances of AD and AE changed by up to 2 % due to impact at 5 J. This indicated that there is a critical thickness at which the current sensing system cannot be used to detect damage.

Through – thickness electrical resistivity of carbon fibre composite laminates was inversely proportional to laminates thicknesses as presented in Section 3.1. Through – thickness current density decreased when the composite cross section area increased, this means the sensitivity of the current sensing system decreased. To investigate the suitability this sensing system to detect damage in thick CFRP laminates, 2.54 mm and 3.5 mm panels were subjected to 10 J of impact energy. The electrical resistance changed by only 7% in 2.54 mm panel

and 3.8% in 3.5 mm panel as shown in Figure 10.

In order to make the process economically viable, electrical contacts would need to be widely spaced so the effect of the sensor size and spacing between electrodes on the sensitivity of the technique was studied. Figure 12 shows data from using sensing mat 2 (which has larger and more widely spaced contacts than mat 1) to collect electrical resistance data. In sensing mat 2 the electrode area was 400 mm^2 and the distance between electrodes was 90 mm. At a given impact energy the change in electrical resistance using sensing mat 2 in all panels was less than the change in electrical resistance using sensing mat 1 as shown in Figure 10 and Figure 12. In fact, when 1 J caused damage of 61.60 mm^2 in 0.84 mm panel, this damage caused a measurable electrical resistance change using mat 1 (the damage was detectable), however, it was not detectable when mat 2 was used.

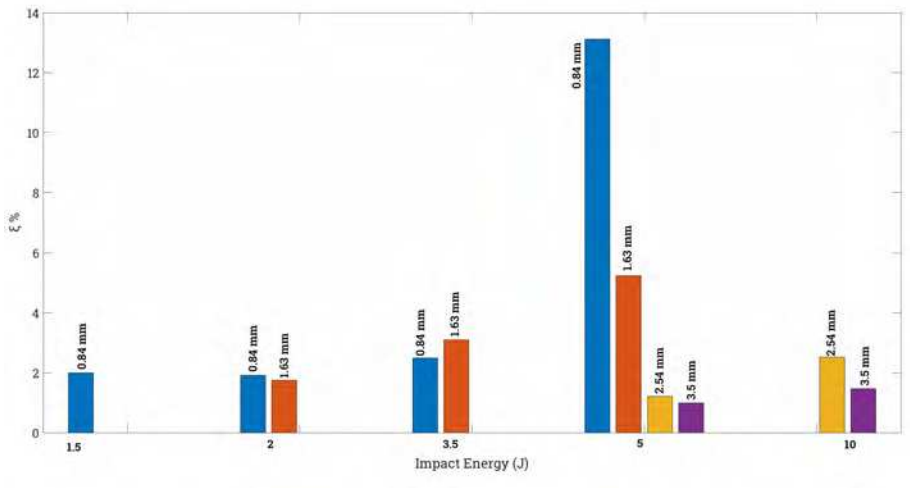

Figure 12: The percentage change in electrical resistance in carbon fibre composite laminate panels due to impact damage using sensing mat 2. Number on the bars represent panel thicknesses.

3.3. Damage Location

The main advantage of this technique was the ease with which the damage can be located. This technique had an advantage over C-scan in that it

located the damage area within few seconds (in principle electrical resistance measurements were virtually instantaneous so large area scans could be completed in milliseconds although the current system takes several seconds to cycle through consecutive measurements), C-scan is by its nature a slow process. An individual four-probe electrical resistance measurement cannot map the damage (while C-scan does that in 2D and 3D) but an array of measurements provided by sensing mats such as used in this work can be combined with some simple data processing to produce a 2D map of damage. The sensing mats divided the CFRP laminate panels into segments as shown in Figure 13, across which the electrical resistances were measured before and after each impact.

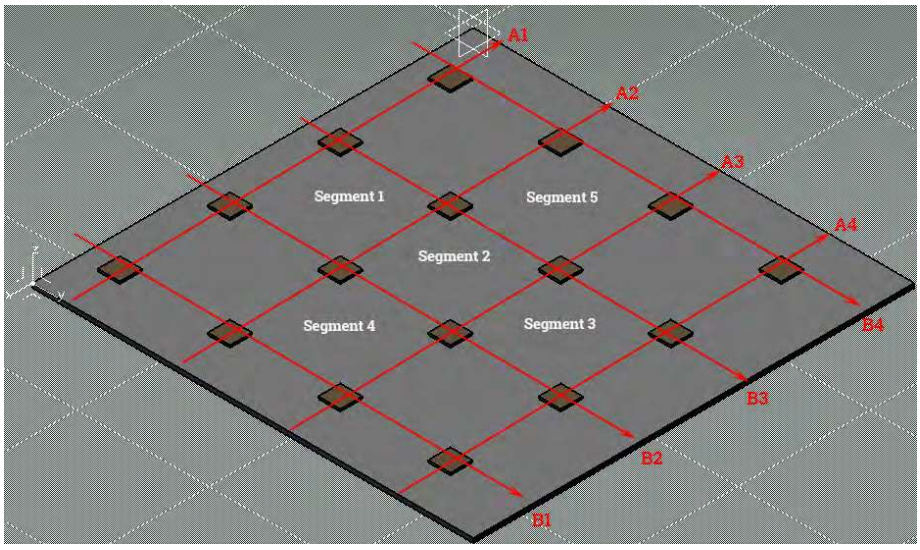

Figure 13: Representation of damage identification technique using electrical resistance change method.

The electrical resistance at each segment was measured and then the electrical resistance changes at each segment were measured again at various impact energies. The electrical resistance readings were analysed by plotting the changes in electrical resistance using Equation 8 against the axis (i.e. A and B) that they were measured at.

$$\Delta R = R_i - R_o \tag{9}$$

Where ΔR is the change in electrical resistance at a segment, R_i is the electrical resistance after impact, and R_o is the electrical resistance before impact 3.2. The damage was located by significant local variations in the electrical resistances occurred in a panel as shown in Figure 14 to Figure 17 . Using this data, maps of the resistance changes can be plotted, giving a 2D view of the resistance profile across the panel, and clearly facilitating the identification and location of damage within the structure. The change in electrical resistance increased when impact energy increased, therefore damage can be located precisely. Figure 14a shows the damage location due to impact event at 1 J, the change in electrical resistance was small and damage was widely spread. When impact energy increased, Figure 14b, c, and d, damage became more localised up until the impact energy increased to 5 J (Figure 14e) where a complete perforation occurred to the panel and the change in electrical resistance became inaccurate due to damage in sensing mats.

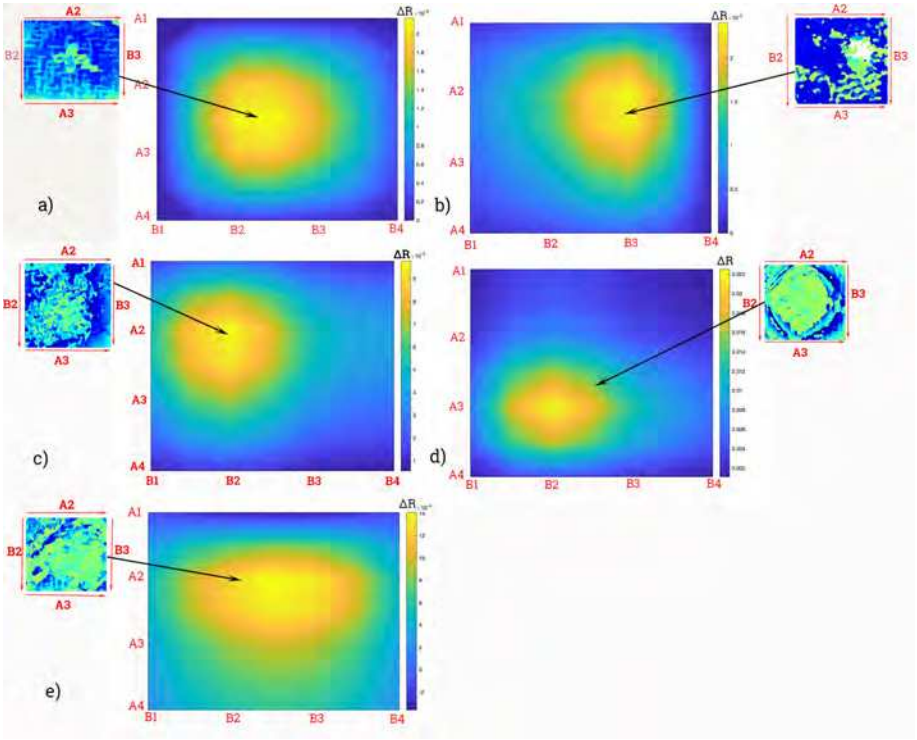

Figure 14: Damage location in 0.84 mm panels that were impacted at various impact energies a) 1 J, b) 1.5 J, c) 2 J, d) 3.5 J, and e) 5 J. The C- scan images at the corners represent the damage profile, and the arrows around C – scan image the current flow direction.

It can also be seen that C-scan images helped to determine damage profiles. The smaller the damage the more spread the contours were. The arrows around C-scan images represented the direction of electrical current applied into the CFRP laminate panels. All panels were impacted in Segment 2 (Figure 13), therefore the highest changes in electrical resistance were occurred in the region between A2, A3, B2, and B3. In spite of the fact that the sensing electrode in this region experienced the highest electrical resistance changes, however the changes in electrical resistance were varied from a sensing electrode to the others. This in turn was shifted damaged areas on the contours from Segment 2 to other segments slightly. This challenge was attributed to amount of electrical contacts made with the carbon fibres in CFRP laminate panels during attaching

the sensing mats to CFRP laminate panels. It is important to state that this type of error was inherited in the electrical resistance sensing technique and it required an advanced signal processing technique to overcome it. When impact energy increased to 5 J, all types of damage were occurred (matrix crack, fibre breakage and delamination), therefore the damaged area was big as shown in Figure 14e.

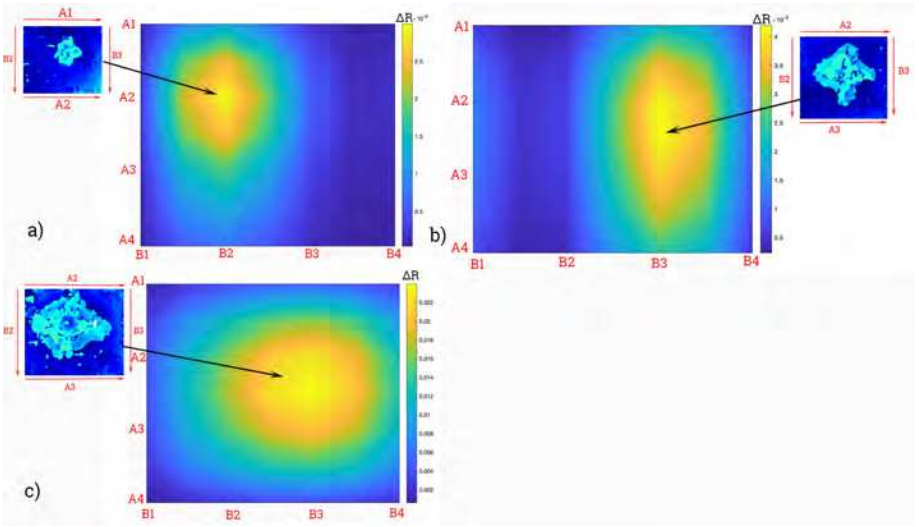

Figure 15: Damage location in 1.63 mm panels that were impacted at various impact energies a) 2 J, b) 3.5 J, and c) 5. The C- scan images at the corners represent the damage profile, and the arrows around C – scan image the current flow direction.

When the thickness of the CFRP laminate panel increased to 1.63 mm (Figure 15), the changes in electrical resistance were less than the CFRP laminate panel in Figure 14. When the thickness increased to 2.54 mm the changes in electrical resistance were as low as $11x10^{-4}$ Ω when the panel impacted at 5 J (Figure 16). However, damage was located, and damage was more localised when the CFRP panel was impacted at 10 J.

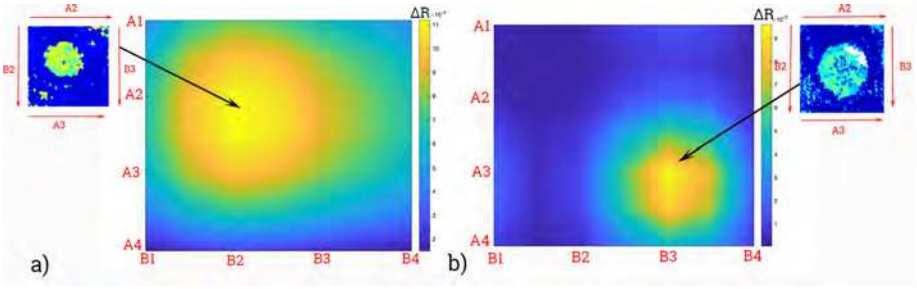

Figure 16: Damage location in 2.54 mm panels that were impacted at various impact energies a) 5 J and b) 10 J. The C- scan images at the corners represent the damage profile, and the arrows around C – scan image the current flow direction.

370 5 J and 10 J impact energies caused BVID in 3.5 mm CFRP laminate panel; the changes in electrical resistance was as low as $3.5x10^{-4}$ and $2.5x10^{-3}$ Ω respectively. It can be concluded that fibre volume fraction has higher impact on the electrical resistance sensing system than panel thick-nesses.

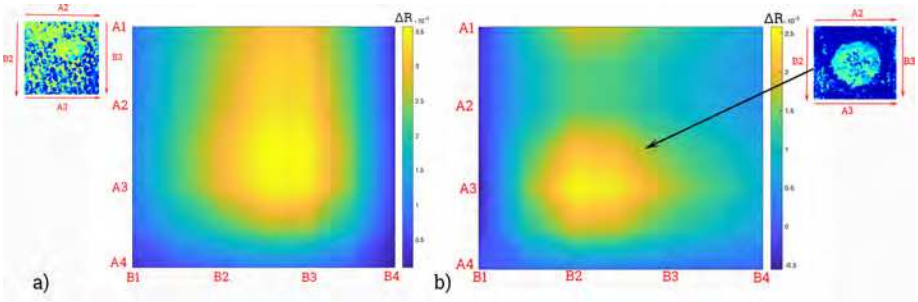

Figure 17: Damage location in 3.5 mm panels that were impacted at various impact energies a) 5 J and b) 10 J. The C- scan images at the corners represent the damage profile, and the arrows around C – scan image the current flow direction.

4. Conclusions

375 This study has proved that the electrical resistance sensing system can be used to detect and locate damage in *woven fabric* CFRP laminate panels. The main benefit of the current sensing system is that the ease with which the damage can be located due to the innovative sensing mats and the simple analytical

methods used. It was found that the sensitivity of the sensing system was a function of carbon fibre volume fraction, panel thickness, damage severity and the electrode surface area and spacing. The electrical resistance baseline is affected by surface area of the sensing electrodes more than other factors. It has been found that increasing the surface area of the electrode from $100mm^2$ to $400mm^2$ and the spacing between electrodes from $40mm$ to $90mm$ increased the baseline electrical resistance by up to 55%. This implies that the distance between electrodes has higher effects than the surface area of the sensing electrodes on damage detection. It was also expected that increasing the thickness of the CFRP panels will increase the electrical resistivity of the panels where the current flows through a greater distance, however the thicker the CFRP panels the higher the carbon fibre volume fraction and the lower the electrical resistivity. This in turn means that carbon fibre volume fraction has greater effect on the electrical resistivity than the thickness of the CFRP panels.

Acknowledgements

I would like to acknowledge the financial contribution of the Higher Committee for Education Development in Iraq (HCED) for making this work possible

References

[1] R. Salvado, C. Lopes, L. Szojda, P. Araújo, M. Gorski, F. J. Velez, J. Castro-Gomes, R. Krzywon, Carbon fiber epoxy composites for both strengthening and health monitoring of structures, Sensors 15 (5) (2015) 10753–10770.

[2] D. R. Cramer, D. F. Taggart, H. Inc, Design and manufacture of an affordable advanced-composite automotive body structure, in: Proceedings of the 19th International Battery, Hybrid and Fuel Cell Electric Vehicle Symposium & Exhibition, 2002.

[3] D. Chung, Damage detection using self-sensing concepts, Proceedings of

the Institution of Mechanical Engineers, Part G: Journal of Aerospace Engineering 221 (4) (2007) 509–520.

[4] Y. Y. Lim, S. Bhalla, C. K. Soh, Structural identification and damage diagnosis using self-sensing piezo-impedance transducers, Smart Materials and Structures 15 (4) (2006) 987.

[5] J. M. Brownjohn, Structural health monitoring of civil infrastructure, Philosophical Transactions of the Royal Society of London A: Mathematical, Physical and Engineering Sciences 365 (1851) (2007) 589–622.

[6] W. Liu, B. Tang, Y. Jiang, Status and problems of wind turbine structural health monitoring techniques in china, Renewable Energy 35 (7) (2010) 1414–1418.

[7] W. Staszewski, C. Boller, G. R. Tomlinson, Health monitoring of aerospace structures: smart sensor technologies and signal processing, John Wiley & Sons, 2004.

[8] S. Rana, R. Fangueiro, Advanced composite materials for aerospace engineering: Processing, properties and applications, Woodhead Publishing, 2016.

[9] R. D. Finlayson, M. Friesel, M. Carlos, P. Cole, J. Lenain, Health monitoring of aerospace structures with acoustic emission and acousto-ultrasonics, Insight-Wigston then Northampton- 43 (3) (2001) 155–158.

[10] B. Hofer, Fibre optic damage detection in composite structures, Composites 18 (4) (1987) 309–316.

[11] W. Staszewski, S. Mahzan, R. Traynor, Health monitoring of aerospace composite structures–active and passive approach, composites Science and Technology 69 (11-12) (2009) 1678–1685.

[12] D. C. Betz, G. Thursby, B. Culshaw, W. J. Staszewski, Acousto-ultrasonic sensing using fiber bragg gratings, Smart Materials and Structures 12 (1) (2003) 122.

[13] W. Roundi, A. El Mahi, A. El Gharad, J.-L. Rebiere, Acoustic emission monitoring of damage progression in glass/epoxy composites during static and fatigue tensile tests, Applied Acoustics 132 (2018) 124–134.

[14] P. Shrestha, Y. Park, C.-G. Kim, Low velocity impact localization on composite wing structure using error outlier based algorithm and fbg sensors, Composites Part B: Engineering 116 (2017) 298–312.

[15] M. Krishnapillai, R. Jones, I. Marshall, M. Bannister, N. Rajic, Thermography as a tool for damage assessment, Composite structures 67 (2) (2005) 149–155.

[16] J. S. Leng, A. Asundi, Real-time cure monitoring of smart composite materials using extrinsic fabry-perot interferometer and fiber bragg grating sensors, Smart materials and structures 11 (2) (2002) 249.

[17] M. LeBlanc, et al., Impact damage assessment in composite materials with embedded fibre-optic sensors, Composites Engineering 2 (5-7) (1992) 573–596.

[18] A. Ciliberto, G. Cavaccini, O. Salvetti, M. Chimenti, L. Azzarelli, P. Bison, S. Marinetti, A. Freda, E. Grinzato, Porosity detection in composite aeronautical structures, Infrared physics & technology 43 (3-5) (2002) 139–143.

[19] K. Schulte, , C. Baron, Load and failure analyses of cfrp laminates by means of electrical resistivity measurements, Composites science and technology 36 (1) (1989) 63–76.

[20] A. Todoroki, K. Omagari, Y. Shimamura, H. Kobayashi, Matrix crack detection of cfrp using electrical resistance change with integrated surface probes, Composites science and technology 66 (11-12) (2006) 1539–1545.

[21] T. Swait, F. Jones, S. Hayes, A practical structural health monitoring system for carbon fibre reinforced composite based on electrical resistance, Composites Science and Technology 72 (13) (2012) 1515–1523.

[22] R. J. Hart, O. Zhupanska, Influence of low-velocity impact-induced delamination on electrical resistance in carbon fiber-reinforced composite laminates, Journal of Composite Materials (2018) 0021998318776361.

[23] A. Todoroki, M. Tanaka, Y. Shimamura, Measurement of orthotropic electric conductance of cfrp laminates and analysis of the effect on delamination monitoring with an electric resistance change method, Composites Science and Technology 62 (5) (2002) 619–628.

[24] A. Todoroki, Y. Tanaka, Y. Shimamura, Delamination monitoring of graphite/epoxy laminated composite plate of electric resistance change method, Composites Science and Technology 62 (9) (2002) 1151–1160.

[25] P. Irving, C. Thiagarajan, Fatigue damage characterization in carbon fibre composite materials using an electrical potential technique, Smart materials and structures 7 (4) (1998) 456.

[26] J. Wen, Z. Xia, F. Choy, Damage detection of carbon fiber reinforced polymer composites via electrical resistance measurement, Composites Part B: Engineering 42 (1) (2011) 77–86.

[27] S. Wang, D. Chung, Self-sensing of flexural strain and damage in carbon fiber polymer-matrix composite by electrical resistance measurement, Carbon 44 (13) (2006) 2739–2751.

[28] N. Angelidis, C. Wei, P. Irving, The electrical resistance response of continuous carbon fibre composite laminates to mechanical strain, Composites Part A: applied science and manufacturing 35 (10) (2004) 1135–1147.

[29] X. Wang, D. Chung, Self-monitoring of fatigue damage and dynamic strain in carbon fiber polymer-matrix composite, Composites Part B: Engineering 29 (1) (1998) 63–73.

[30] J. Gadomski, P. Pyrzanowski, Experimental investigation of fatigue destruction of cfrp using the electrical resistance change method, Measurement 87 (2016) 236–245.

[31] J. Abry, Y. Choi, A. Chateauminois, B. Dalloz, G. Giraud, M. Salvia, In-situ monitoring of damage in cfrp laminates by means of ac and dc measurements, Composites Science and Technology 61 (6) (2001) 855–864.

[32] R. Schueler, S. P. Joshi, K. Schulte, Damage detection in cfrp by electrical conductivity mapping, Composites Science and Technology 61 (6) (2001) 921–930.

[33] M. Zappalorto, F. Panozzo, P. A. Carraro, M. Quaresimin, Electrical response of a laminate with a delamination: modelling and experiments, Composites Science and Technology 143 (2017) 31–45.

[34] G. Schoeppner, S. Abrate, Delamination threshold loads for low velocity impact on composite laminates, Composites Part A: Applied Science and Manufacturing 31 (9) (2000) 903 – 915. doi:https://doi.org/10.1016/S1359-835X(00)00061-0.
URL http://www.sciencedirect.com/science/article/pii/S1359835X00000610